The Theory of Risk Uncertainty Reduction

by Robert W. L. Thomas, Marilyn J. Eichelberger and Missey Lee Dahlgren, Virginia

The objective of this research is to examine the character of safety programs in not only reducing risk, but also in reducing relative risk uncertainty. This paper approximates the distributions of both the probability and severity of a mishap as lognormal and examines the likely behavior of the co-distribution as the safety process is executed. This paper also shows how differential forces across the risk plane reduce both the risk itself and the relative uncertainty in the risk at the same time. With this new approach, risk now becomes a quantitative item with a known probability distribution, providing a new metric for safety program effectiveness.

Introduction

This paper attempts to mathematically model risk, severity and probability. Such an attempt may be difficult for all system safety programs [Ref. 1], given the complexity of risk and its elements as defined in MIL-STD 882E [Ref . 2]. In our earlier work [Refs. 3-5], the distribution of mishap probability was characterized given a combination of practical experience, simulation-based testing and the incorporation of expert opinion. Here, we add mishap consequence considerations, and define the risk plane as the graph of consequence, or severity, as a function of mishap probability. Risk is the product of probability and severity. At the 2017 International System Safety Conference (ISSC), Zito [Ref. 6] suggested approximating the distributions of both the probability and severity of a mishap as lognormal. In this paper, we examine the likely behavior of the co-distribution of probability and severity as the risk reduction process is executed. We review the expected motivations in different parts of the risk plane during the safety program and show that they will reduce both the risk itself and the relative uncertainty in the risk at the same time.

First, we discuss appropriate scaling for the probability-severity graph, and then examine the validity of the lognormal approximation for the mishap probability distribution by comparison with the known exact beta distribution [Refs. 3-5, 9]. Next, we consider the validity of lognormal distribution as a descriptor of mishap severity, based on an examination of actual insurance claim data [Ref. 11], and review the strength of motivations in the different regions of the probability-severity plane. This leads naturally to the compression and distortion of the risk zone as the safety process is executed to reduce the risk, with a related reduction in risk uncertainty.

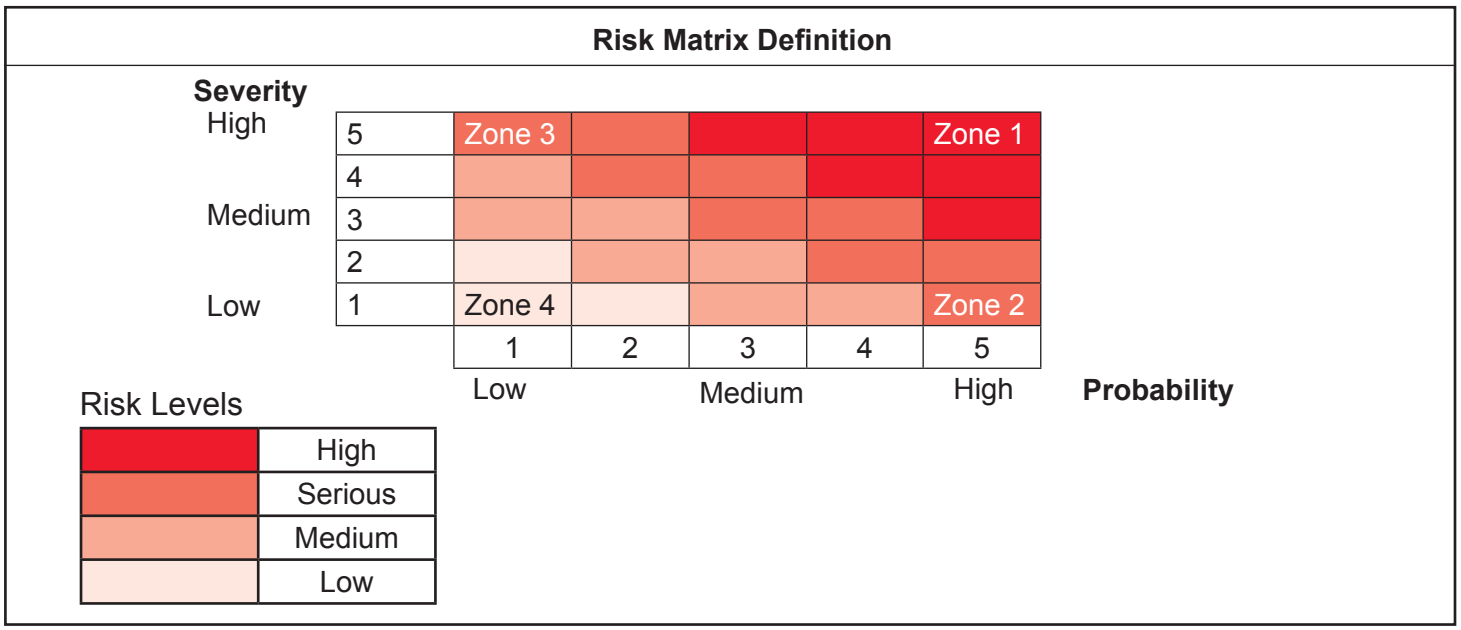

Figure 1 — Risk Matrix Definition for This Study.

This is followed by an example to show how a safety program's success can be assessed using actual mishap data. We consider a safety improvement program for a hypothetical sports car, generating simulated data for miles covered since the last accident and the claim amount, both before and after the implementation of the safety program. The appropriate statistical metrics for program assessment are developed.

Finally, we consider the similarity between the safety risk plane and the performance risk plane, and show that the same representation and statistical functionality apply to both cases. Thus, it is likely that the concepts described here can be applied universally to both systems safety [Refs. 1, 7] and systems engineering [Ref. 8].

For this effort, we created a definition of the risk plane as illustrated in Figure 1. This risk matrix differs from the matrix given in MIL-STD 882E [Ref. 2]. In this case, the severity of the mishap increases vertically, while the mishap probability increases horizontally. In an earlier standard [Ref. 7], the levels separating the regions were given numerically, but these values have been omitted from more recent standards [Ref. 1], as they can be tailored to the scope of the particular risk levels for the subsystem under consideration. For example, most developed sedentary occupations present a very small fatality risk, but that may not be the case for jobs in mobile systems, such as vehicles.

In Figure 1, risk increases from the bottom left to the top right of the diagram, with correspondingly increased risk and seniority requirements for approval. Initially, it is difficult to assess which zone is appropriate for the system under consideration as the data available is limited, with a related uncertainty in the required level of authority. As the safety process proceeds, data collected and expert judgment will result in reducing risk uncertainty.

Risk Plane Representation

In this paper, we limit ourselves to a quantitative definition of risk, which for this paper is defined as financial. Figures 2a and 2b are strictly conceptual. They show lines of constant risk on the risk plane using linear and log scaling, respectively. As you will see, the relative risk is reduced when we examine the distortion of the confidence regions of the risk plane in log-log, rather than in a linear scale. Note that the lines of constant risk in the log-log plot are straight lines, indicating a fractal behavior [Ref. 9]. This shows that if we work within the log-log context, our methods and conclusions can be applied at all problem scales, from very small risks to very large risks. In the case of a single safety incident,

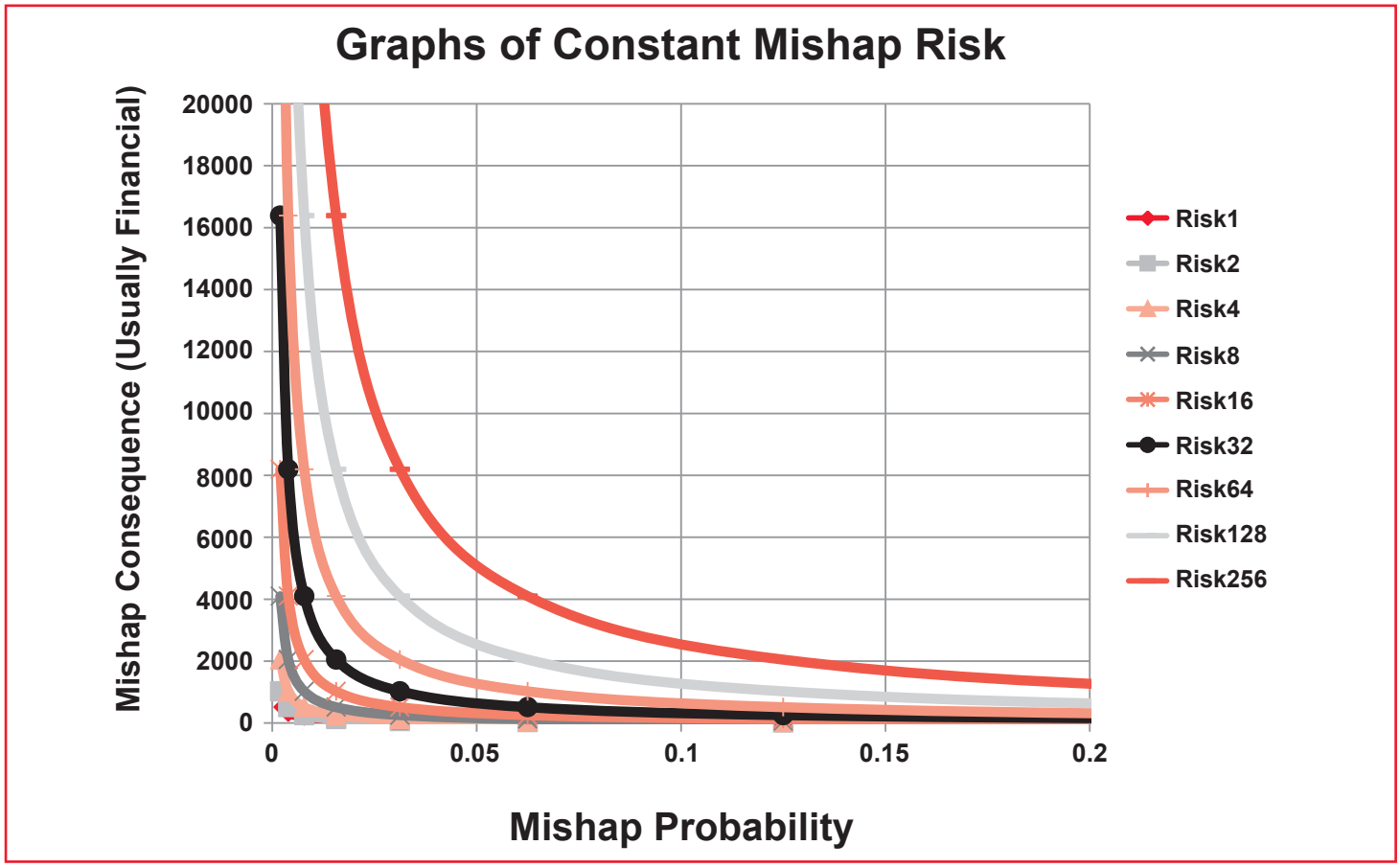

Figure 2a — Lines of Constant Risk (Linear Scale).

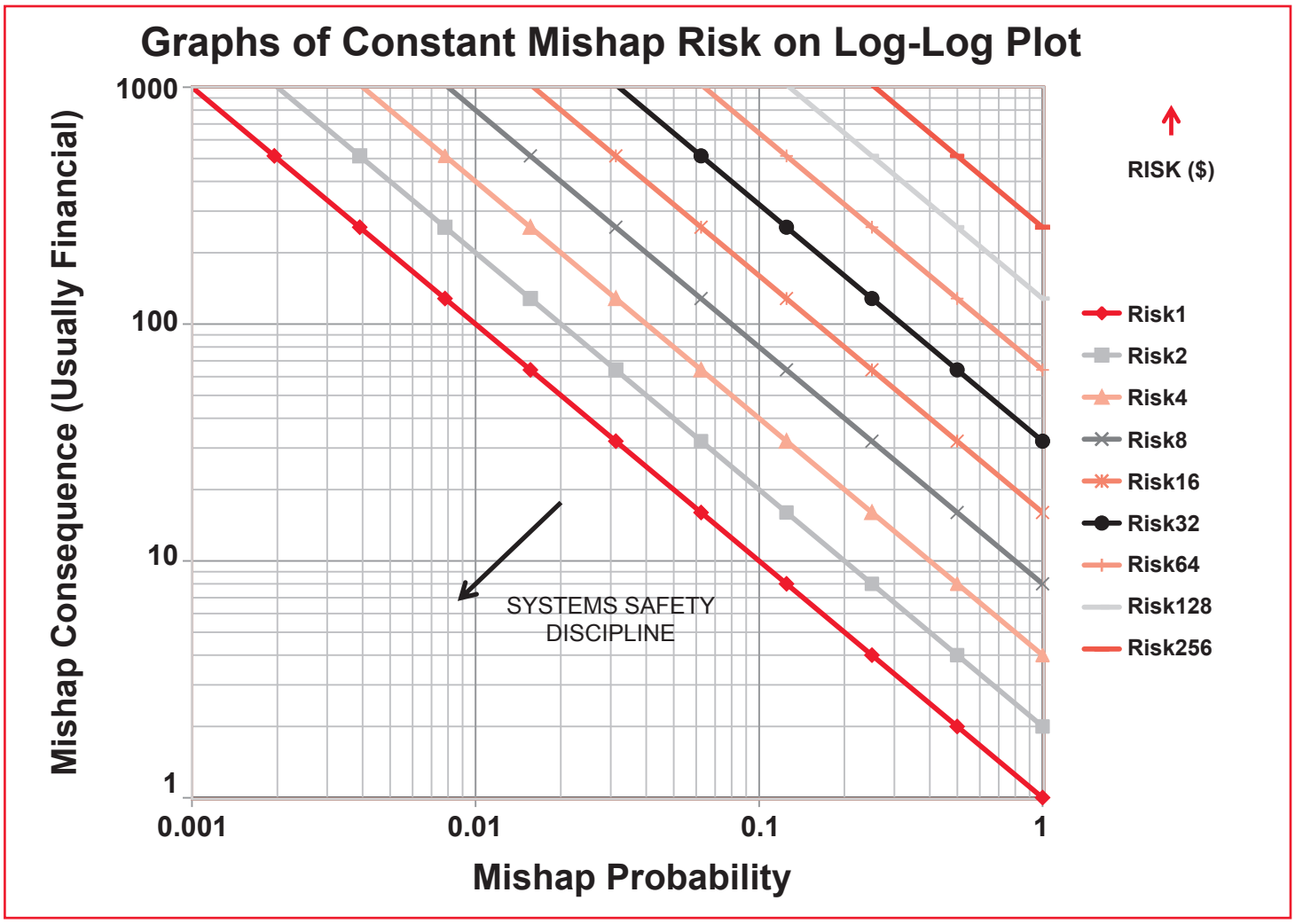

Figure 2b — Lines of Constant Risk with Log-Log Scaling.

the probability cannot be greater than 1. However, engineers usually normalize probability to a unit of time, distance or given number of products; for example, in this case, the probability is not bounded. One of the goals of any safety program is to reduce risk, and this is illustrated by the arrow shown in Figure 2b. To demonstrate this, we must identify the uncertainty distributions in the risk plane, both before and after any risk reduction effort.

Uncertainty Distributions

To compute the distribution of risk uncertainty, we need to know the distributions of the uncertainties in the risk factors, probability and severity of a mishap. We know that the exact form of the distribution of the mishap probability based on testing experience is beta [Ref. 10], so our first task is to evaluate how closely the lognormal form approximates the beta distribution. To do this, the following equations are used to compute the median and shape parameters, μ and σ, respectively, of the lognormal distribution from the number of observed failures, n, in N tests, through the intermediate parameters, m and V, which are the mean and variance parameters of the beta distribution.

If we have a lognormal distribution for the probability, $p = \exp(\mu + \sigma Z)$, where μ is the median parameter, σ is the shape parameter, and Z is a Normally distributed number with zero mean and a standard deviation of 1. For any data set, we can compute the mean, m and variance, V, and then calculate the following values of the median and shape parameters:

$$\mu = \ln[m/\sqrt{(1 + V/m^2)}] \quad (1)$$

$$\sigma = \sqrt{[\ln(1 + V/m2)]} \quad (2)$$

For a situation where we observe n failures in N trials, we can obtain m and V uniquely as follows:

$$m = (n+1)/(N+2) \quad (3)$$

$$V = (n+1).(N-n+1)/[(N+2)2.(N+3)] \quad (4)$$

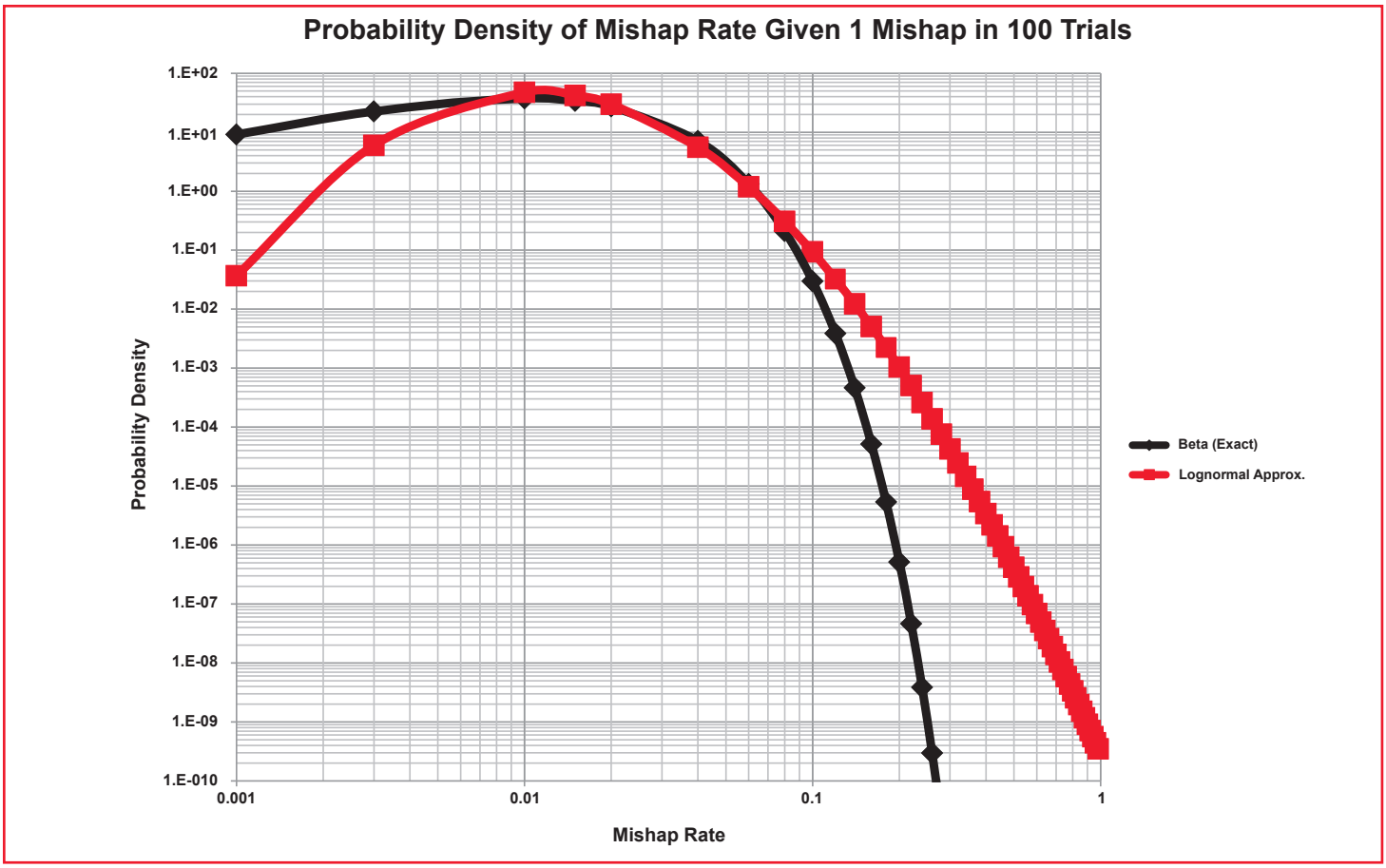

Figure 3a — Lognormal Approximations for n=1 and N=100.

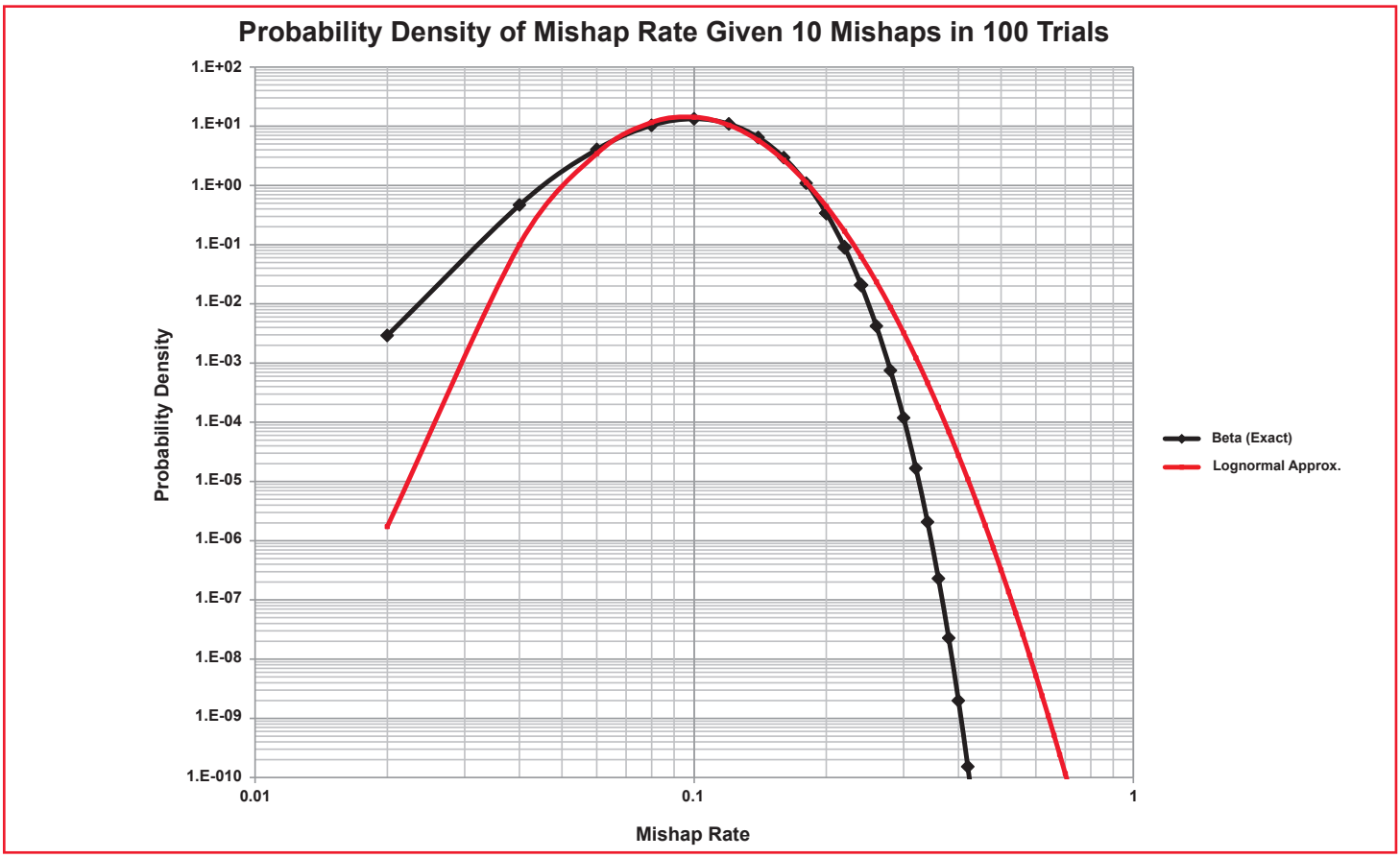

Figure 3b — Lognormal Approximations for n=10 and N=100.

For complex systems, we derive n and N through simulations combined with expert opinions [Ref. 5]. For simple systems with low consequences, diligent data collection can be used to obtain n and N directly. While equations 1 through 4 are non-linear, they are, at least, monotonic, so there will be a unique solution. Figures 3a and 3b give the comparison of the exact beta distribution with the lognormal approximation for N=100 and n=1 and 10, respectively. Since the mean and variance of the distributions have been set to be equal, the differences come in at the level of the third moment, i.e., the average of the cube of the displacement from the mean, or skewness. When a lognormal distribution is plotted against a logarithmic scale, the result has zero skewness, since the skewness of a Normal distribution is zero. Through inspection, we see that the beta distribution has negative skewness when using a logarithmic scale, which is not surprising as the beta distribution is defined only up to a probability of one. It follows that the approximation underestimates the number of small probabilities and overestimates the number of large probabilities, and is therefore conservative.

We now examine the distribution of mishap severity. In Figure 4, Achieng [Ref. 11] has shown that while the lognormal model was by no means a perfect fit, it was reported to be the best option of all models tried when using insurance claim data for automobile accidents. The detailed distributions will depend on the specific character of the possible mishap types, of course, but the lognormal form seems to work well over many types.

Finally, we assess the uncertainty distribution of the risk itself. Since the product of two log-normally distributed numbers is also lognormal, the risk distribution may be approximated reasonably accurately as lognormal. The parameters, μ and σ, can be estimated from those of its associated probability and severity distributions. This calculation requires us to include a correlation coefficient if it is non-zero.

As mentioned above, the risk is the product of the mishap probability and the mishap severity, so

$$\text{Log(Risk)} = \text{Log(Probability)} + \text{Log(Severity)}$$
$$\text{or } L_R = L_P + L_S \quad (5)$$

The variance in the logarithm of the risk is

$$V(L_R) = V(L_P) + V(L_S) + 2*\text{Corr}(L_P,L_S)*\sqrt{(V(L_P)V(L_S))} \quad (6)$$

showing that negative correlation between probability and severity reduces risk uncertainty.

Confidence Regions in the Risk Plane

Figure 5 shows the expected character of confidence regions in the risk plane before and after a risk reduction effort.

Shown is a schematic illustration of the initial and final confidence zones before and after the execution of a safety improvement program. Note that on a log-log plot, the confidence regions for bi-lognormal distributions appear to be bi-normal, so they are ellipses with 95 percent confidence regions about twice the size of the 68 percent distributions with co-aligned axes. If the initial confidence zone shows little correlation between probability and confidence, the probability distribution of the mishap probability will be independent of the severity level.

We now examine the distribution of expected forces on the confidence region during a safety improvement program, and the net effect of forces from opposing corners of the risk plane. This is detailed in the following paragraphs.

In the top right corner of Figure 5, there is a strong motivation to reduce both the probability and

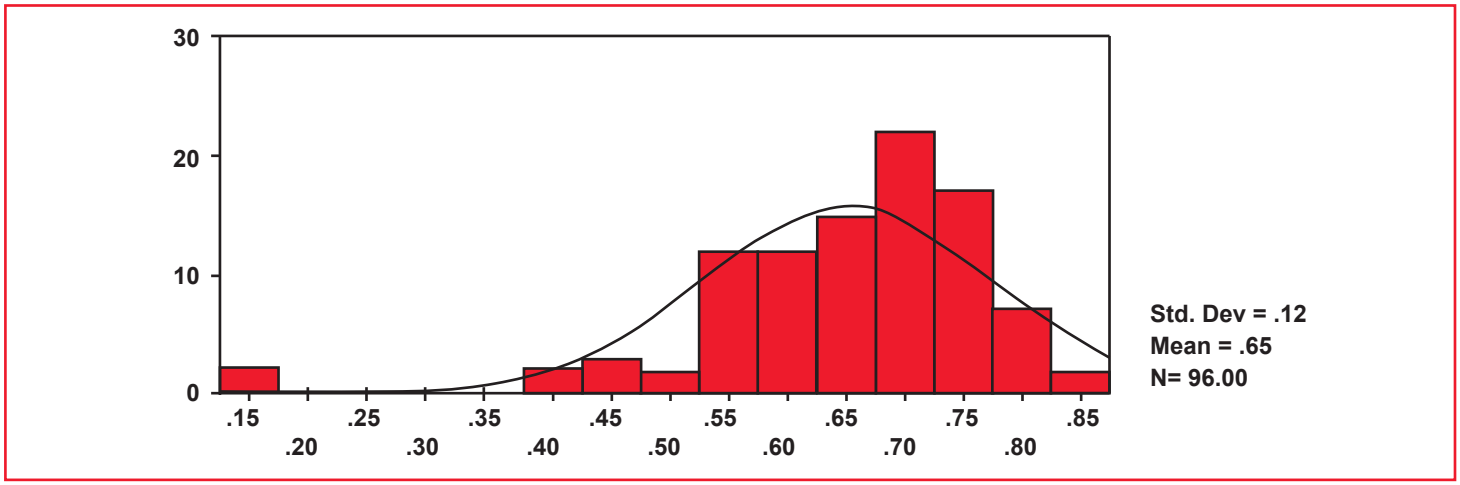

Figure 4 — Example of Fit of Lognormal Distribution to Actual Insurance Claims Frequency.

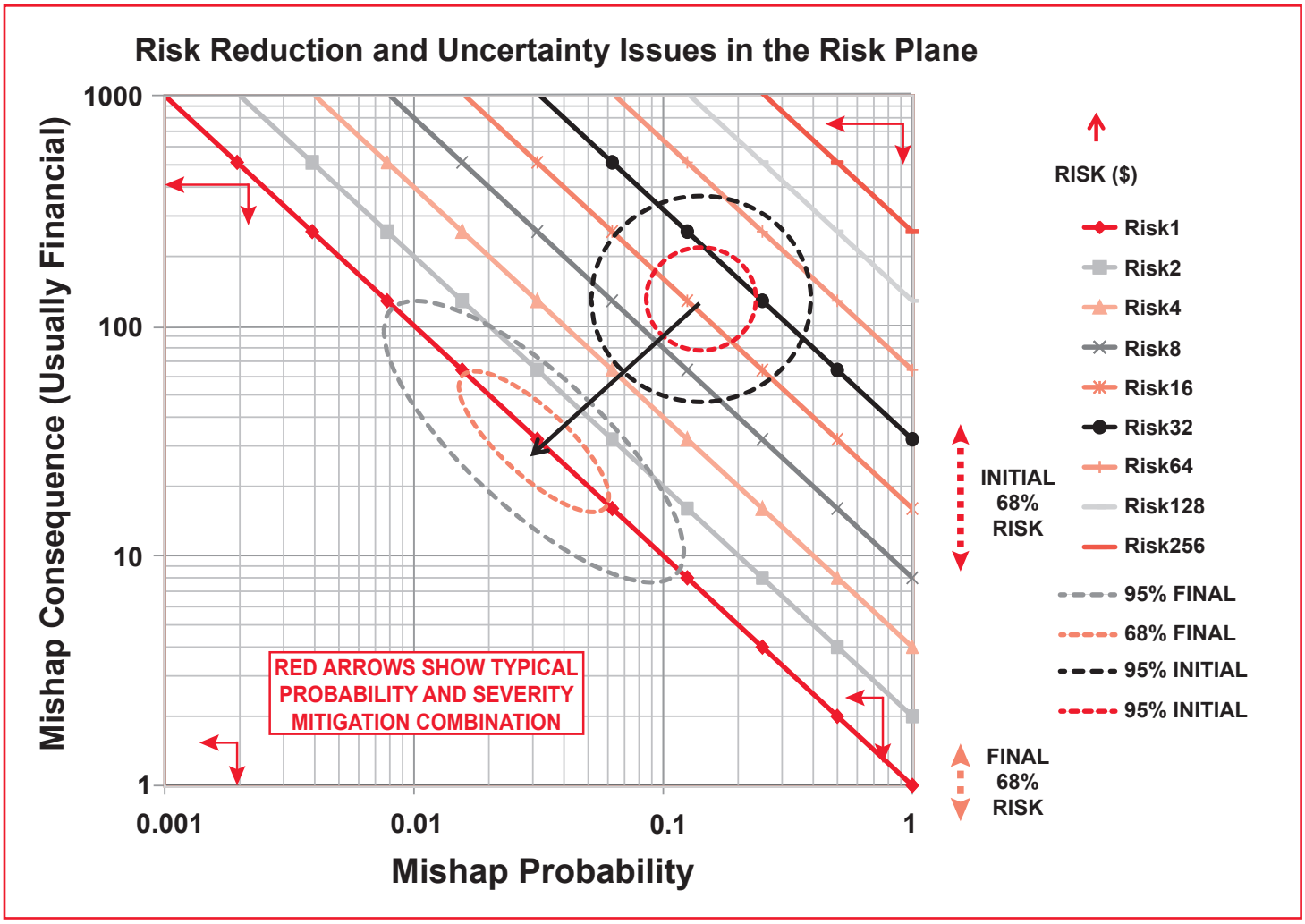

Figure 5 — Confidence Regions in the Risk Plane Before and After Safety Program Implementation.

the consequence, since both are unacceptably high. In the bottom left corner, however, there is little motivation to reduce either probability or consequence since both are acceptably low. The net effect of these forces is to compress the confidence region in the direction of decreased risk as the mean risk itself is reduced. Note that the mishap probability distribution now depends on the severity, and the median probability is inversely proportional to the median severity.

In the top left corner of Figure 5, there is a high mishap consequence, but a low mishap risk. This might correspond to a fatality, where the cost is always high. In this case, all we can do is add extra barriers to reduce the likelihood, and the net force on the confidence region is to the left. In the bottom right corner, we have high probability mishaps with low consequences. Examples include paper cuts or parking lot bumps. In this case, our best course of action is to mitigate the consequences, such as improving the quality and distribution of first aid kits or providing free cans of touch-up paint. The net effect of these forces is to stretch the confidence region along the line of constant risk so that negative correlation is introduced to the confidence region, resulting in reduced relative error in the risk as shown.

This entire discussion can be applied as is to performance risk uncertainty reduction, with the caveat that "mishap" is reinterpreted as "performance failure."

A Specific Simulation Showing the Type of Validating Data Required for our Theory

We consider an example of data collected before and after an accident risk reduction program for a hypothetical sports car. Improvements have been divided into two columns in Figure 6, with those on the left designed to reduce accident probability, and those on the right reducing consequences of an accident, s, in thousands of dollars. Data collected before and after the ac-

Accident Risk Reduction Program for Sports Car	
Accident *Probability* Mitigation	**Accident *Consequence* Mitigation**
• Blind spot visual monitors	• Passenger cage stiffening
• Automatic braking	• Crumple zone redesign
• Back-up camera	• Additional airbags
• Audio proximity warning	• Interior padding improvements
• Lane tracking devices	• Re-anchoring of seatbelts
• Increased running light power	• Firewall updates
• Improved traction tires	• Automatic fire extinction
• Blind spot radar sensors	• Electronic collision reporting

Figure 6 —Accident Risk Reduction Program for Sports Car.

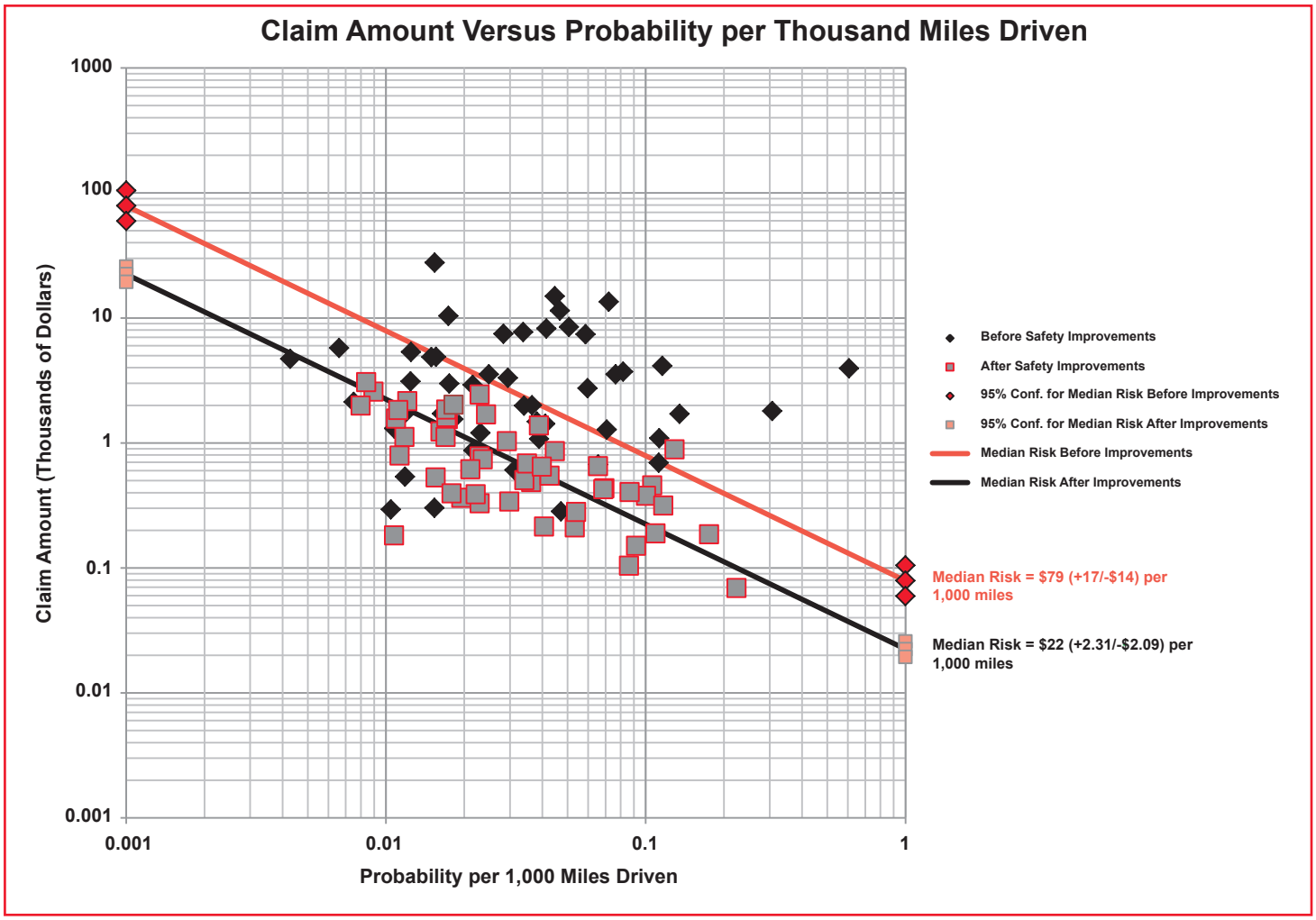

Figure 7 — Graphs of Accident Severity versus Probability Before and After Safety Improvement Program.

cident includes miles driven since the previous accident and the amount of the claim. Mileage was divided into 1,000 to estimate the accident rate, p, per thousand miles driven. We then graphed severity as a function of probability, as shown in Figure 7, for 50 simulated accidents both before and after the implementation of the safety program.

For each point, risk is calculated as the product of the probability and severity, and constant risk lines were drawn corresponding to the median risk for each case. Prior to the improvement program, the median accident risk per thousand miles driven was $79 (+$17/-$14), while after the program, the value was only $22 (+$2.3/-$2.1). Note that the uncertainties

in the positive and negative directions are unequal, due to the lognormal distribution of risk. The lognormal shape factor in the median was reduced by the program from 0.2 to 0.1, giving double the relative confidence in the computed risk. The risk shape factors for the total populations resulted in a reduction from 1.4 to 0.7. The 95 percent confidence zones drawn at the ends of the median constant risk graphs are, in fact, twice as large as the range given by the standard errors.

Conclusions

We have developed a general theory of uncertainty in mishap risk, and shown that it is likely that the safety discipline will result in a reduction in the relative uncertainty in risk as the risk itself is reduced. The best statistical model approximates both mishap probability and severity as lognormal, resulting in a lognormal distribution of risk. With this new approach, risk now becomes a quantitative item with a known probability distribution, providing a new metric for safety program effectiveness. The conclusions for the safety risk also apply to performance risk because the safety and performance risk planes have identical characterizations.

About the Authors

Dr. Robert W. L. Thomas is a scientist at AECOM working on safety issues pertaining to electromagnetic environments near to high-power emitters. He also has experience with the verification and validation of combat systems software with a particular emphasis on critical-timing issues. He has also developed models used by the National Aeronautics and Space Administration (NASA) to scope the independent verification and validation of satellite- and spacecraft-borne software and has designed optical instrumentation for space measurements to characterize planetary atmospheres.

Marilyn J. Eichelberger is currently a member of the Combat Systems Safety Branch at the Naval Surface Warfare Center, Dahlgren Division. She has 21 years of experience supporting U.S. Navy, U.S. Marine Corps and foreign military programs, of which eight years have been in the role of Principal for Safety.

Missey Lee is currently a member of the Combat Systems Safety Branch at the Naval Surface Warfare Center, Dahlgren Division. She has more than 11 years of experience practicing system safety engineering for the U.S. Navy. Previously, she developed and implemented code for Weapon Systems of the U.S. Navy.

References

1 Kady, R.A., A. Ranasinghe, M.G. Zemore and R.A. Eller. "The Challenges of a Quantitative Approach to Risk Assessment," Proceedings of the 32nd International System Safety Conference, St. Louis Missouri, August 4-8, 2014.

2 Military Standard 882E. "System Safety," May 11, 2012, http://www.system-safety.org/Documents/MIL-STD-882E.pdf , retrieved March 24, 2016.

3 Thomas, R.W.L., M. Eichelberger, M. Lee and J. Haan. "An Innovative Approach to Hypothesis Testing for System Safety Assessment," Proceedings of the 33rd International System Safety Conference, San Diego, California, August 21-24, 2015.

4 Thomas, R.W.L., M. Eichelberger, M. Lee, and J. Haan. "An Innovative Approach to Hypothesis Testing for System Safety Assessment," *Journal of System Safety*, Fall 2015, 18-23.

5 Thomas, R.W.L., M. Eichelberger and M. Lee. "Setting Testing Requirements for Simulation Based System Safety Assessments," Proceedings of the 34th International System Safety Conference, Orlando, Florida, August 8-12, 2016.

6 Zito, Richard R. "How Complex Systems Fail III: The System Risk Surface", Proceedings of the 34th International System Safety Conference, Orlando, Florida, August 8-12, 2016.

7 Military Standard 882C. "System Safety," May 11, 2012, http://www.system-safety.org/Documents/MIL-STD-882C.pdf, retrieved March 24, 2016.

8 Military Standard 881C, "Work Breakdown Structures," October 3, 2011, http://www.mcri.com/wp-content/uploads/2014/09/Military-Standard-881C-----Department-of-Defense-Standard-Practice-----Work-Breakdown-Structures-for-Defense-Materiel-Items-MIL-STD-881C-3-Oct-11.pdf, retrieved March 24, 2016.

9 Boeing, G. "Visual Analysis of Nonlinear Dynamical Systems: Chaos, Fractals, Self-Similarity and the Limits of Prediction," http://www.mdpi.com/2079-8954/4/4/37, retrieved May 2, 2017.

10 Navarro, Daniel and Amy Perfors. "An Introduction to the Beta-Binomial Model," http://compcogscisydney.org/ccs/technote_betabinomial.pdf, retrieved May 22, 2018.

11 Achieng, O.M. "Actuarial Modeling for Insurance Claim Severity in Motor Comprehensive Policy Using Industrial Statistical Distributions," http://zorig.gigfa.com/actuarial-modeling-insurance-claim-severityin-motor-comprehensive-policy/?i=1, retrieved May 22, 2018.